Received: 2 May 2022 | Revised: 15 February 2023 | Accepted: 19 April 2023

DOI: 10.1002/gdj3.207

Geoscience Data Journal RMetS WILEY

DATA ARTICLE

Surface water quality in Amazonian Floodplain Lakes, data set of the Lago Grande de Curuai Floodplain Lake, Pará-Brazil

Derlayne Dias Roque[1] | **Marie-Paule Bonnet**[2,3,4] | **Jérémie Garnier**[1,3,4] | **Cleber Kraus Nunes**[3,4,5] | **Patrick Seyler**[3,4] | **David Motta Marques**[3,4,6]

[1]Instituto de Geociências, Universidade de Brasilia, Brasilia, Brazil

[2]Espace-DEV, IRD, University of Montpellier, Montpellier, France

[3]LMI OCE, IRD, Universidade de Brasilia, Brasilia, Brazil

[4]INCT ODISSEIA, Universidade de Brasilia, Brasilia, Brazil

[5]Instituto Nacional de pesquisas espacias, Sao jose do Campos, Brazil

[6]Instituto de Pesquisas Hidráulicas, Universidade do Rio Grande Sul, Porto Alègre, Brazil

Correspondence
Marie-Paule Bonnet, Espace-DEV, IRD, University of Montpellier, Montpellier, France.
Email: marie-paule.bonnet@ird.fr

Funding information
Conselho Nacional de Desenvolvimento Científico e Tecnológico, Grant/Award Number: 465483/2014-3 and 490634/2013-3; Fondation pour la Recherche sur la Biodiversite, Grant/Award Number: Clim-FABIAM

Abstract

Between 2013 and 2017, we carried out nine field missions in the Lago Grande de Curuai floodplain, located in Pará state – North of Brazil – to collect samples for monitoring surface water quality. This site separated from the river by a narrow bank is composed of a network of channels and shallow lakes, a morphology shared by the floodplains of the lower Amazon. A multiparameter probe was used *in situ* to measure electrical conductivity, temperature, pH, dissolved oxygen, chlorophyll, turbidity, depth and a Secchi disk to estimate transparency. Water grab samples were analysed for suspended material, alkalinity, humic acid, phosphorus, nitrogen, carbon and chlorophyll. Sampling stations were distributed over the seven larger lakes in the floodplain and sampled at different periods of the hydrological cycle. The number of samples varied with the floodplain water level, with a minimum of 25 samples for each field visit. This data set is a collection of water quality data to assist in the limnological or biogeochemical studies of surface waters in Amazonian floodplain lakes, and the product of successive French-Brazilian projects: (1) the Clim-FABIAM 'Climate changes and Floodplain lake biodiversity in the Amazon Basin: how to cope and help the ecological and economic sustainability' funded by the French Foundation for biodiversity research (FRB), (2) the project Bloom-ALERT –'Environmental sensitivity and population health vulnerability to cyanobacteria in the Amazon:

Dataset

Identifier: https://doi.org/10.23708/SNGQHV

Creators: Derlayne Dias Roque, Marie-Paule Bonnet, Jérémie Garnier, Cleber Kraus Nunes, Patrick Seyler, David Motta Marques

Data set correspondence: marie-paule.bonnet@ird.fr

Title: Surface water quality (2013–2017) – Curuai floodplain, Brazil, Pará

Publisher: DataSuds

Publication year: 2023

Resource type: observational data

Version: V1.

towards shared indicators' funded by the French-Brazilian research program GUYAMAZON 2014, and the project (3) 'Ecossistemas das várzeas e biodiversidade: Impactos das mudanças ambientais e climáticas considerando cenários de desenvolvimento sustentáveis' (Project number 490634/2013-3) funded by the Brazilian National scientific Research Council CNPq.

KEYWORDS

Amazon River, floodplain, water quality, wetlands

1 | INTRODUCTION

Wetlands and floodplain habitats host exceptional biodiversity levels and provide numerous ecosystems services for human societies, such as nutrient recycling, groundwater recharge and flood regulation. Driven by human population growth and economic expansion, their global extent has been drastically reduced, with a loss of about 87% since the beginning of the eighteenth century (Davidson, 2014). As he reported, the rate of wetland loss is 3.7 times faster during the twentieth and twenty-first centuries. Natural wetlands and floodplains are now among the most endangered ecosystems in the world (IPBES, 2019).

In the Amazon basin, floodplains and associated wetlands form a vast and complex mosaic covering about 14% of the total basin area ($5.83.10^6 km^2$), including permanent water (Hess et al., 2015). Ongoing changes in the basin such as deforestation, expansion of agriculture and cattle ranching, mining activities, road construction, the installation of dams along the rivers and global warming are threats for these environments (Castello & Macedo, 2016). The floodplains and wetlands of the lower Amazon have been particularly impacted, mainly due to deforestation linked to the jute trade, followed by cattle ranching and the expansion of soybean fields (Renó et al., 2011). However, the intention shared by several bordering countries to significantly increase the production of electric energy through the construction of several hydroelectric reservoirs in the watershed is of particular concern for all of these environments (Forsberg et al., 2017; Latrubesse et al., 2017, 2020).

Appraising the combined impact of these changes remains a challenging task because knowledge and data on these environments remain scarce, widely dispersed across the basin (Castello & Macedo, 2016), and data sets rarely made available to the scientific community, especially regarding the water quality. To the best of our knowledge, only very few *in situ* water quality data sets have been published or made available to the scientific community to date. The Large-Scale Biosphere-Atmosphere Experiment in Amazonia (LBA) program published several data sets on the basin. Part of these data sets focus on water quality in the Amazon River or floodplains and GHG emissions. For instance, the 'LBA-ECO LC-07 reflectance spectra and water quality of Amazon basin floodplain lakes' data set (https://doi.org/10.3334/ORNLDAAC/1144) covers a portion of the central amazon (bounding rectangle −2.96 N; −3.98 S; −60.53 E; −63.90 W) for the July and August 2000 (Novo & Melack, 2013). The Pre-LBA Carbon in the Amazon River experiment (CAMREX) data (https://doi.org/10.3334/ORNLDAAC/904) covers a 2000-km-long reach along the mainstream with data acquired during 13 cruises organized at contrasting hydrological periods over the period 1982–1991.

This paper presents the water quality data set produced between 2013 and 2017 by three research projects: (1) the Clim-FABIAM 'Climate changes and Floodplain lake biodiversity in the Amazon Basin: how to cope and help the ecological and economic sustainability' funded by the French Foundation for biodiversity research (FRB) through its call 'Modelling and biodiversity scenarios', 2011, the project (2) Bloom-ALERT –'Environmental sensitivity and population health vulnerability to cyanobacteria in the Amazon: towards shared indicators' funded by the French-Brazilian research program GUYAMAZON 2014 and the project (3) 'Ecossistemas das várzeas e biodiversidade: Impactos das mudanças ambientais e climáticas considerando cenários de desenvolvimento sustentáveis' (Project number 490634/2013–3) funded by the Brazilian National scientific Research Council CNPq.

These projects were conducted within the framework of the International Mixed Laboratory (LMI/OCE) of *Universidade de Brasília and IRD*. They were carried out in partnership between several institutions; in France: *Institut de Recherche pour le Développement* (IRD) and *Centre de Coopération Internationale en Recherche Agronomique pour le développement* (CIRAD); in Brazil: *Laboratório de Geoquímica* (LAGEQ) of *Universidade de Brasília* (UnB), *Divisão de Sensoriamento Remoto* (DSR) of *Instituto Nacional de Pesquisas Espaciais* (INPE), *Universidade Federal de Goiás* (UFG), *Instituto de Pesquisas Hidráulicas* (IPH) of *Universidade Federal do Rio Grande do Sul* (UFRGS), *Universidade do Estado*

do Amazonas (UEA), *Universidade Federal do Oeste do Pará* (UFOPA) and *Universidade Federal de Juiz de Fora* (UFJF).

The data set contains water quality data from 50 different sites well distributed over the lakes of a representative floodplain of the low course of the Amazon, the Lago Grande de Curuai (LGC) Floodplain (bounded rectangle −01°50′16″ N – 02°15′12″ S and −55°00′51″ E – 56°05′00″ W), resulting from nine cruises over the period 2013–2017 at contrasting hydrological periods. It includes two types of data sets files. One file provides records for the 30 water quality parameters analysed (pH, temperature, total suspended solids, Secchi depth, dissolved oxygen and conductivity), nutrients (N, P), organic carbon chlorophyll-a, sample depth and total depth for all cruises. For each cruise, a second file contains the vertical measurement profiles obtained at the different sampling stations by a multiparameter probe (EXO-2 probe equipped with temperature, pH, optical dissolved oxygen, turbidity, chlorophyll-a and conductivity sensors) calibrated regularly onboard the vessel.

The data set is available at https://doi.org/10.23708/SNGQHV (DataSuds repository, IRD).

The data set has already been used, at least in part, in the fields of ecology, biology and geosciences, by masters and Ph.D. students involved in the projects (Bomfim, 2017; Dias-Roque, 2022; Gomes et al., 2020; Kraus, 2015, 2019; Lobo, 2016; Reis, 2017; Lobo, 2021) and a few publications (Bomfim et al., 2019; Câmara dos Reis et al., 2019; Kraus et al., 2019, 2021; Lobo et al., 2018).

The data set contains rare information on the region, particularly on floodplain ecosystems, and we believe it represents a significant contribution to the scientific community in Limnology. It can also support analyses in the field of remote sensing to help for the calibration of satellite products aimed at characterizing chlorophyll or suspended matter from reflectance analysis. Finally, it is also an interesting water quality benchmark in these environments.

2 | THE LAGO GRANDE DE CURUAI FLOODPLAIN

The LGC Floodplain is a 120-km-long/40 km-wide floodplain segment (−01°50′16″ N – 02°15′12″ S and −055°00′51″ E – 056°05′00″ W), Pará State, Brazil located on the southern margin of the Amazon River, in front of the town of Óbidos and 900 km upstream from Atlantic Ocean (Figure 1). The floodplain represents the lower Amazon River's floodplains, composed of sedimentary landforms with large shallow lakes separated by narrow levees from the main river course (Rudorff et al., 2014a). Small channels connect lakes to each other and the main river permanently or temporarily, depending on the hydrological period (Bonnet et al., 2008).

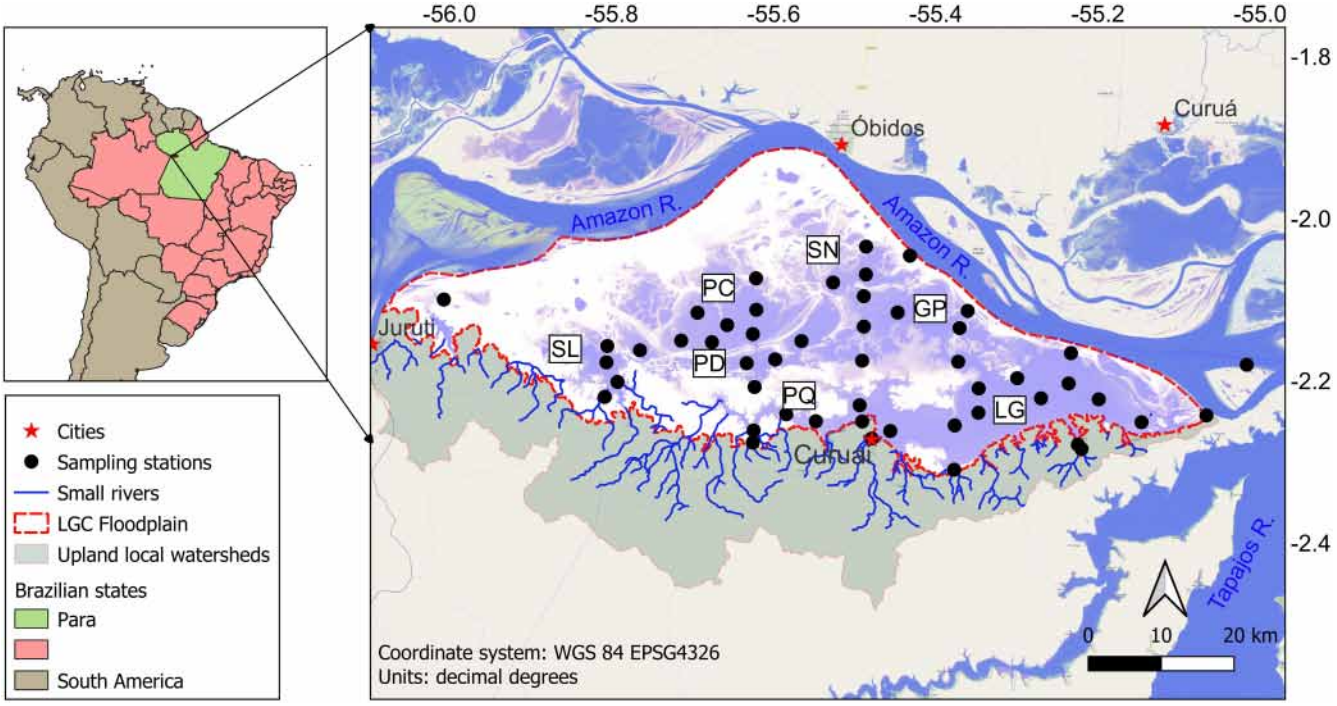

FIGURE 1 Study area – Lago Grande de Curuai Floodplain. Water bodies: LG: Lago Grande; GP: Grande Poção; PC: Poção; PD: Piedade; PQ: Piracuará; SN: Santa NInha; SL; Salé; Standard open street map and the Global surface water occurrence map (Pekel et al., 2016) are used as background.

The average seasonal variation of the water level in the floodplain is 6 m over the last two decades, which results in a considerable variation of the extension of the inundated areas from 575 to 2090 km^2. This extent represents about 13% of the total area flooded between Manaus and Óbidos (Bonnet et al., 2016; Rudorff et al., 2014b). It is classical to decompose the hydrograph in four periods. The flood peak is usually reached in June and lasts a few days, and the receding waters are from June to October. The low-water period is reached during November, and the rising period is from December to May.

The local drainage area, extending over 1,370 km^2 to the south, covers several basins drained by small Igarapé streams (Bonnet et al., 2008). Based on a classification of a Landsat image, (Peres et al., 2018) show that this region was covered by approximately 48% primary forest, 33% secondary vegetation, 13% pasture and 3% cropland in 2014. The two other classes considered (urbanized area and savannah) occupy less than 3%.

Bonnet et al. (2008); Rudorff et al. (2014b) provided a detailed analysis of the LGC floodplain water balance over the 1997–2003 and 1995–2010 periods respectively. Both studies calculate the respective contributions of mainstream water, local runoff, direct rainfall and seepage to the floodplain water balance during each hydrological cycle. The Amazon River inflow is the main contribution to the floodplain water mixture, varying between 77% and 82% depending on the period and study. Direct precipitation and local runoff account for about 20% of total inputs and groundwater seepage less than 5%. Strong interannual variations are noted in these two studies, with, for example, inflows from the river that can be ninefold between the driest (1997) and the wettest (2009) years over the period 1995–2010 (Rudorff et al., 2014b). The mean residence time of the water within the floodplain is estimated to be around 3 months (Bonnet et al., 2008).

The primary LGC floodplain water input is from the Amazon River, so it receives large inputs of white water, rich in nutrients and suspended material. However, our work shows that the water quality of the lakes is quite different from that of the Amazon River, outside of the peak flood period. Regarding suspended solids, (Bourgoin et al., 2007; Rudorff et al., 2018) proposed a study of suspended sediment balance, respectively, over 2000–2003 and 1995–2014. (Bourgoin et al., 2007) report an average value of the input sediment flow of 1,512 ± 9 Gg/year and the output flows of 802 ± 9 Gg/year, which corresponds to the storage of 710 ± 19 Gg, that is, 47% of the input flow. The values reported by (Rudorff et al., 2018) are 4088 ± 2017 and 2251 ± 471 Gg/year for input and output, respectively, about 40% higher than the values proposed by the previous study, but the storage remains in the same order with a value of 44%. The differences between the two studies can be explained on the one hand by the method of calculation, the flows calculated by (Rudorff et al., 2018), take into account more precisely the contributions by overflow, and on the other hand, by an intensification of the water river-floodplain exchanged flows, with a succession of important floods since 2005. Both studies indicate that the floodplain exports sediment late during the receding period (especially from September to November) due to wind-induced sediment resuspension.

The nutrients and chlorophyll-a concentrations over the floodplain present substantial variations linked to phytoplankton primary production (Alcântara et al., 2008; Kraus et al., 2019). The phytoplankton is partly responsible for the considerable variation of particulate organic carbon composition observed along the hydrological cycle (Moreira-Turcq et al., 2013).

3 | SAMPLING AND ANALYTICAL METHODS

3.1 | Monitoring projects and sampling stations

Limnological monitoring for five consecutive years was carried out through three Franco-Brazilian research projects as mentioned above, keeping the same sampling and analysis protocols. The monitoring project began in March 2013 and ended in October 2017, totalling nine field missions with almost 400 superficial water samples. The total amount of valid data *per* parameter is described in Table 1 (data with values below the detection limit were removed from this count).

The LGC floodplain monitoring network consisted of about 50 sampling stations (Figure 1). Sampling stations were selected to represent the area best, considering the seven larger lakes, distributions and characteristics, connections, proximity to upland and the four water periods (rising water stage, high-water stage, receding water stage and low-water stage). At each sampling station, we carried out a vertical profile of *in situ* measurements of the physicochemical variables (temperature, conductivity, pH, turbidity, chlorophyll-a and dissolved oxygen), depth and GPS position or a point sub-surface measurement when the depth was <50 cm. The measurements were carried out with an EXO-2 multiparameter probe daily calibrated. At all sampling stations, water was collected from the subsurface (0.2–0.5 m from the surface) and, for a subset of stations, from different depths with a Van Dorn bottle and stored in 1 L precleaned (washed with 10% HCL and three times rinsed with MilliQ water in the laboratory)

TABLE 1 Amount of valid data *per* parameter.

Parameters	Amount of data	Parameters	Amount of data	Parameters	Amount of data
pH	364	TOC	349	P total	349
Temperature	355	POC	325	P orthophosphate	117
Conductivity	363	DOC	349	P organic	244
ODO	345	AH – 250 nm	349	N total	349
ODO_sat	345	AH – 254 nm	349	N total dissolved	349
Turbidity	343	AH – 365 nm	349	N- ammoniaNH_4^+	300
Chlorophyll	345	AH – 430 nm	349	N-NO_3^- nitrate	265
Alkalinity	298	AH – 750 nm	322	Chlorophyll a	340
Secchi	283			Chlorophyll b	223
SPM	378			Chlorophyll c	274
Silica	349			Pheophytin a	264

low-density polyethylene (LDPE) bottles. The bulk water samples were divided into two parts: one part processed and analysed in the ship's laboratory immediately after collection, and one part was frozen for analysis in the laboratories (*Instituto de Geociências*, *UnB*; *Instituto de Pesquisas Hidráulicas*, *UFRGS*).

Given the operational organization, samples were collected in each survey within 8–12 days from the boat. The ship's laboratory, maintained at 20°C, had an essential working structure on a bench divided into stations for immediate sample filtration, analyses of in-situ parameters (e.g. alkalinity), samples conditioning and freezing. Waters were rapidly filtered after sampling, and both unfiltered and filtered samples were stored at −10°C or 4°C until analysis in laboratories (Ship's UnB and UFRGS laboratories).

3.2 | Analytical methods

In each of the sampling stations, the methodological procedures were applied according to the flow chart of Figure 2.

3.2.1 | Field measurements and laboratory analysis

Each morning, before deploying the multiparameter probe (EXO-2), temperature, pH, conductivity, oxygen concentration/saturation (ODO/ODO_SAT), turbidity and chlorophyll sensors were calibrated with standard methods. The probe was deployed once the boat was anchored in order to avoid too important drifts with the current. This equipment allowed the collection of data in the depth profile at each sampling station. The Secchi disk was used to measure the depth of transparency.

3.2.2 | Laboratory analysis

Alkalinity

The Alkalinity (Gran, 1952) was measured through an acidimetric titration following Mackereth et al. (1989) expressed in mg·L^{-1} $CaCO^3$.

Suspended Particulate Materials

Suspended particulate materials (SPM) concentrations were collected using filtration support and previously weighed 0.45 µm filters (Ø47 mm, dried at 100°C), and filtered 250–500 mL of water. The SPM concentration estimation followed APHA. (2012) expressed in mg L^{-1}.

Chlorophyll-a

We filtered three independent 500 mL replicate samples, from each sampling point, in a glass fibre filter (GF/F Filter, Whatman). After filtration, the three filtres were folded and independently wrapped in aluminium foil and frozen until the analysis in the laboratory. Chlorophyll species were 98% extracted cold ethanol (Jespersen & Christoffersen, 1987). Concentrations of chlorophyll-a, chlorophyll-b, chlorophyll-c and pheophytin, were estimated by reading the optical densities at wavelengths 664, 647, 630 and 750 nm (APHA, 2012) on a spectrophotometer Cary UV–VIS, expressed in mg·L^{-1}.

Carbon TOC, POC and DOC

We used raw and filtered samples for carbon species (total organic-TOC, dissolved-DOC and particulate-POC). Between 250 and 500 mL sample volumes were previously filtered through a pre-ignited (at 450°C in a muffle furnace for 1 hr) glass microfibre filter (Whatman, GF/F, 0.7 µm). An auto-sampler fed both types of samples (raw and filtered) into a Total Organic Carbon Analyser (Shimadzu TOC-VCPH analyser), and the carbon content was estimated after combustion at 680°C and compared to

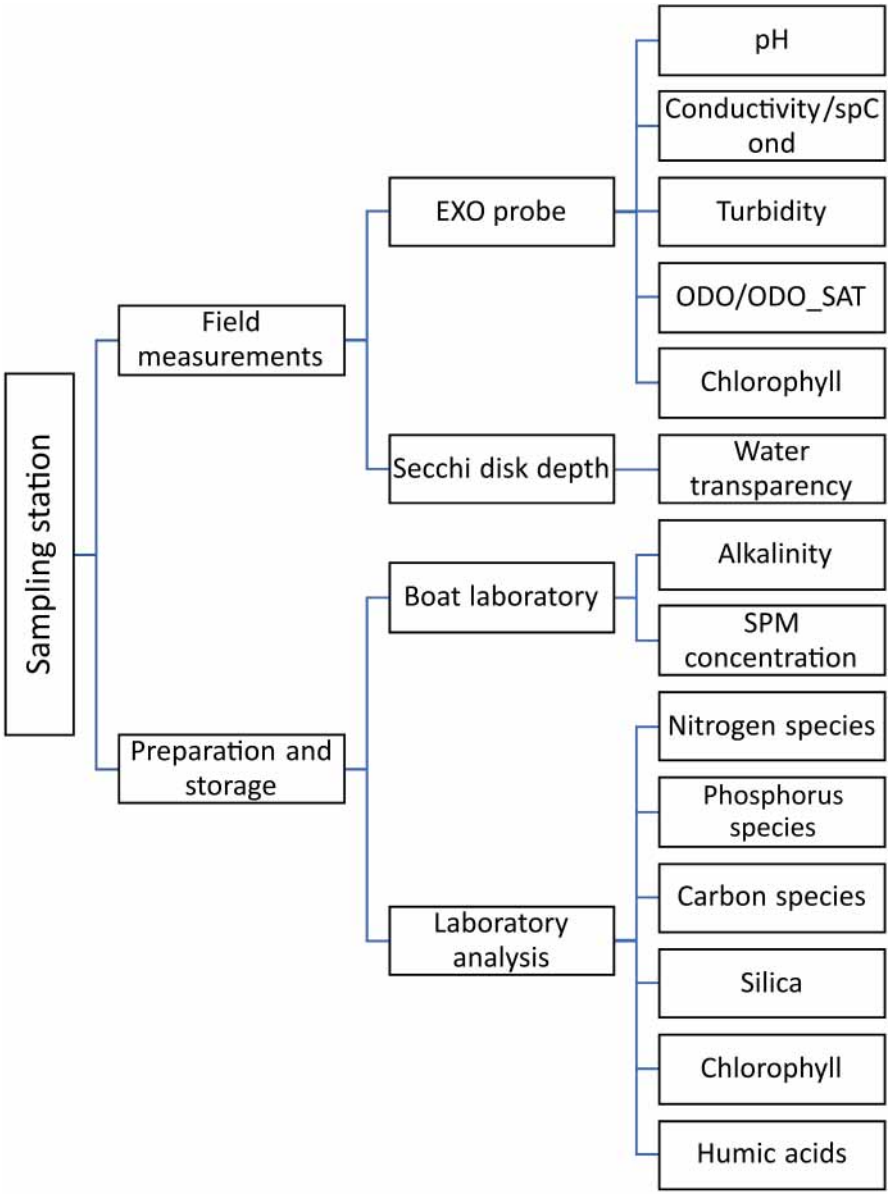

FIGURE 2 Flow chart methodological procedures in all sampling stations.

carbon standards (1–100 mg L^{-1}, Potassium Biphthalate, P.A. Merck), expressed in mg L^{-1} C following the 5,310 methods of total organic carbon (Standard methods www.standardmethods.org).

Nutrients

Nutrients nitrate (mg·L^{-1} NO_3^- -N), ammonium (mg·L^{-1} NH_4^+-N), total phosphorus (mg·L^{-1} PO_4^{-3}-P) and orthophosphate (mg·L^{-1} PO_4^{-3}) were colorimetrically estimated following Mackereth et al. (1989) and APHA (2012) procedures on a Cary UV–VIS spectrophotometer.

Total nitrogen (mg·L^{-1} N) was estimated using raw samples fed by an automated sampler into a coupled Shimadzu TOC-VCPH analyser-Shimadzu Chemiluminescence gas analyser TNM-1, and after sample combustion at 680°C, compared to potassium nitrate standards (0.1–50 mg·L^{-1}, P.A. Merck).

Humic acids

Humic acid concentrations were estimated in filtered samples (Millipore membrane filter, 0.45 µm pore size), following the 5,510 method of aquatic humic substances (Standard methods, www.standardmethods.org) determination. The water absorbance was estimated using a Spectrophotometer Cary UV–VIS, the optical densities were read at 250, 254, 365, 430 and 750 nm wavelengths and expressed in mg·L^{-1}.

Silica

To quantify silicate (SiO_2), we used a photometric method (Si Merck Spectroquant kit for silicates) in filtered samples

(Millipore membrane filter, 0.45 μm pore size) using a Spectrophotometer Cary UV–VIS expressed in $mg \cdot L^{-1}$ S.

3.2.3 | Quality control

Quality control was performed with a reference standard in the procedures. The range and accuracy specifications of EXO-2 multiparameter probe are described in Table 2. At each mission, before starting data collection, the probe's electrodes were calibrated according to the manual and the standards established for each parameter. The data generated from the probe underwent a quality analysis. We excluded data values that did not match the reality of the field, data generated after the probe touched the lake bottom and outliers caused some problems (e.g. dirt on the sensor). The quality of chemical analytical procedures (nutrients, silica and carbon) was checked using certified reference materials.

4 | THE LAGO GRANDE DE CURUAI FLOODPLAIN DATA SET

Data are organized by mission (Table 3), and each mission corresponds to a phase in the hydrological period (Figures 3 and 4). Sampling points located near the margins and temporary islands may vary from the exact location in a radius of up to 0.5 km to the coordinates provided.

At each sampling station, different amounts of analysis were performed. Figure 5 represents the sum of the number of analyses performed by parameters. In the first map, 'all parameters' (Figure 5a) are counted the analyses sums for all parameters. The 'exo profile' (Figure 5b) represents the number of profiles collected for the parameter set: chlorophyll, turbidity, dissolved oxygen, oxygen saturation, temperature, pH and conductivity. The 'physicochemical' (Figure 5c) includes pH, temperature, conductivity, alkalinity, secchi depth and suspended particulate material. The 'phosphorus and nitrogen species' (Figure 5d) include phosphorus (total, orthophosphate and organic) and nitrogen (total, total dissolved, ammonia and nitrate). The 'chlorophyll' (Figure 5e) includes chlorophyll-a, b, c and pheophytin-a. The 'humic acids and organic carbon' (Figure 5f) include humic acids measured at different wavelengths (250, 254, 365, 430 and 750 nm) and organic carbon (total, particulate and dissolved).

5 | POTENTIAL USE OF DATA SET AND RECOMMENDATIONS

Lago Grande de Curuai floodplain is one of the few sites relatively well monitored in the last 30 years. Our data will contribute to enriching the available data on this floodplain and could be used for comparison with other data sets released for this floodplain (Barbosa et al., 2010, data from 2004 to 2006) and also with the data set from other floodplains in the basin or elsewhere in the world (Bonnet et al., 2017; Castillo, 2020; Frappart et al., 2015; Roberto et al., 2009; Rodríguez et al., 2019). It will help monitor potential changes in water quality in these environments while human pressure is increasing rapidly in this region of the world.

These environments are constantly evolving associated with changes in land use and land cover in the hydrographic basin, mainly due to anthropic pressure such as deforestation, construction of dams and use of pesticides in agriculture. Our data will contribute to monitoring possible water quality changes in these environments over time.

TABLE 2 EXO-2 multiparameter probe specifications.

EXO parameters measured	Range	Accuracy	Obs
Chlorophyll	0–400 $\mu g \cdot L^{-1}$ Chl; 0–100 RFU	Linearity: R2 > 0.999 for serial dilution of Rhodamine WT solution from 0–400 $\mu g \cdot L^{-1}$ Chl-*a* equivalent	—
Turbidity	0–4,000 FNU	0–999 FNU: 0.3 FNU or ±2% of reading, w.i.g.; 1,000–4,000 FNU: ±5% of reading	1
Dissolved oxygen	0–50 $mg \cdot L^{-1}$	0–20 $mg \cdot L^{-1}$: ±0.1 $mg \cdot L^{-1}$ or 1% of reading, w.i.g.; 20–50 $mg \cdot L^{-1}$: ±5% of reading	2
Oxygen saturation	0%–500% air saturation	0%–200%: ±1% of reading or 1% saturation, w.i.g.; 200%–500%: ±5% of reading	2
Temperature	−5 to 35°C; 35 to 50°C	±0.01°C; ±0.05°C	3
pH	0–14 units	±0.1 pH units within ±10°C of calibration temp; ±0.2 pH units for entire temp range	4
Conductivity	0–200 $mS \cdot cm^{-1}$	0–100: ±0.5% of reading or 0.001 mS/cm, w.i.g.; 100–200: ±1% of reading	—

Note: 1. Performance-based on 3-point calibration done with YSI AMCO-AEPA standards of 0, 124 and 1,010 FNU. The same type of standard must be used for all calibration points; 2. Relative to calibration gases; 3. Temperature accuracy traceable to NIST standards; and 4. Within the environmental pH range of pH 4–10; More information is available at: https://www.ysi.com/EXO2.

TABLE 3 Sampling mission description.

Mission	Number of samples	Number of sampling stations	Start date (dd/mm/yyyy)	End date (dd/mm/yyyy)	Average level[a] (cm)	Hydrologic phase
FAB I	71	46	08/03/2013	18/03/2013	626	R
FAB II	73	50	08/09/2013	18/09/2013	512	F
FAB III	75	51	27/05/2014	05/06/2014	839	HW
FAB IV	36	36	26/11/2014	03/12/2014	257	LW
FAB V	25	18	05/05/2015	12/05/2015	787	HW
FAB VI	24	24	12/04/2016	21/04/2016	557	R
FAB VII	28	28	29/09/2016	06/10/2016	208	LW
FAB VIII	31	31	11/04/2017	18/04/2017	759	HW
FAB IX	24	24	12/09/2017	18/09/2017	311	F

[a]Average level: average water level read at the 17,050,001 Óbidos-PA gauge during the mission periods. Available on the Hidroweb platform provided by the Brazilian National Water Agency – http://www.snirh.gov.br/hidroweb/serieshistoricas.

Abbreviations: F, flushing period; HW, high water; LW, low water; R, rising period.

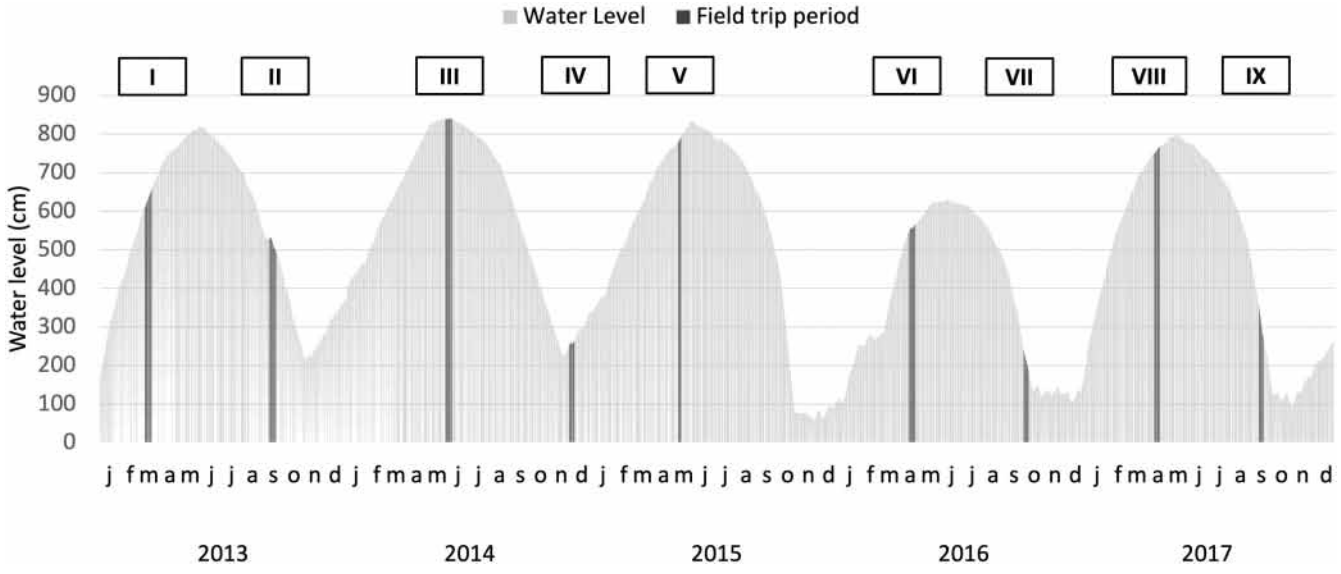

FIGURE 3 Distribution of the field campaigns along the hydrological cycles.

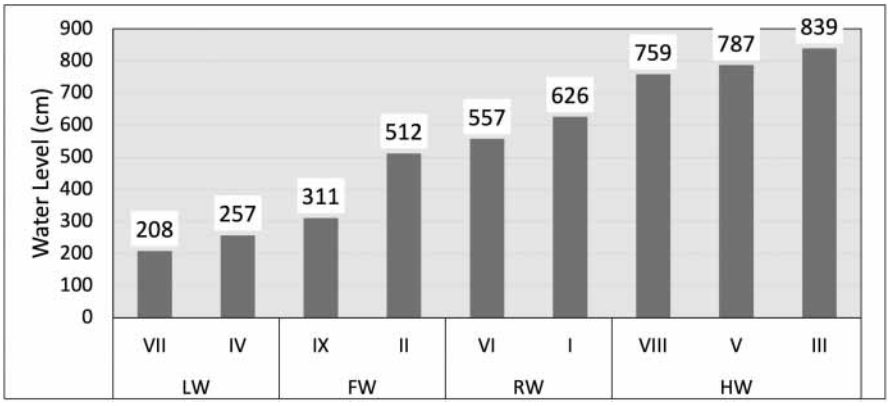

FIGURE 4 Medium water level at each mission; LW, low water; F, flushing; R, rising and HW, high water.

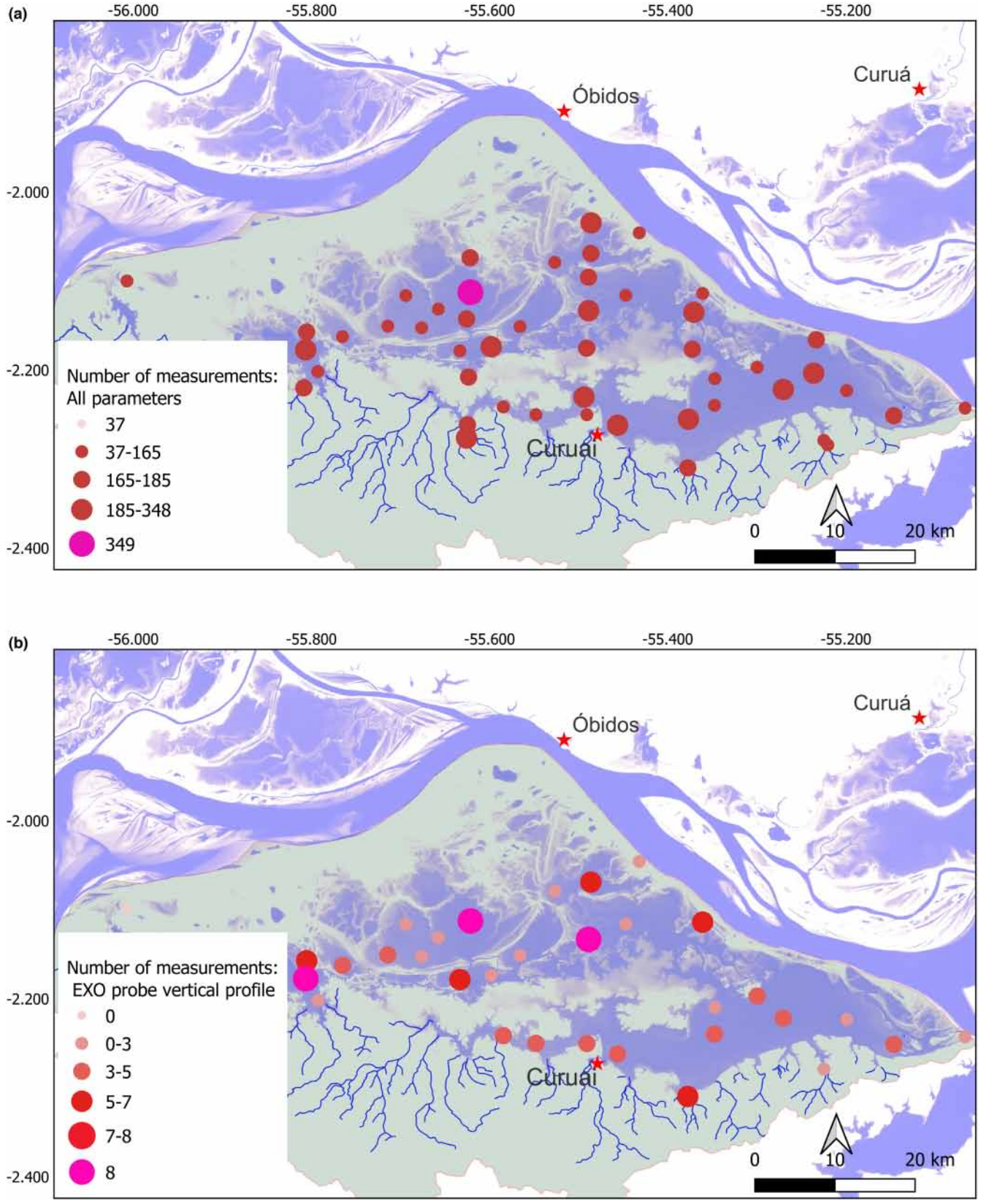

FIGURE 5 Measurements number for all sampling station plotted on LGC floodplain map; (a) all parameters, (b) EXO_profile, (c) physicochemical, (d) humic acids and organic carbon (e) phosphorus and nitrogen species and (f) chlorophyll. For each parameter, the size of the dots and colours of dots, corresponds to the minimum (smallest symbol), maximum (pink symbol) and the sizes of the intervals correspond to the first, second and third quartile. Global surface water occurrence map (Pekel et al., 2016) is used as background.

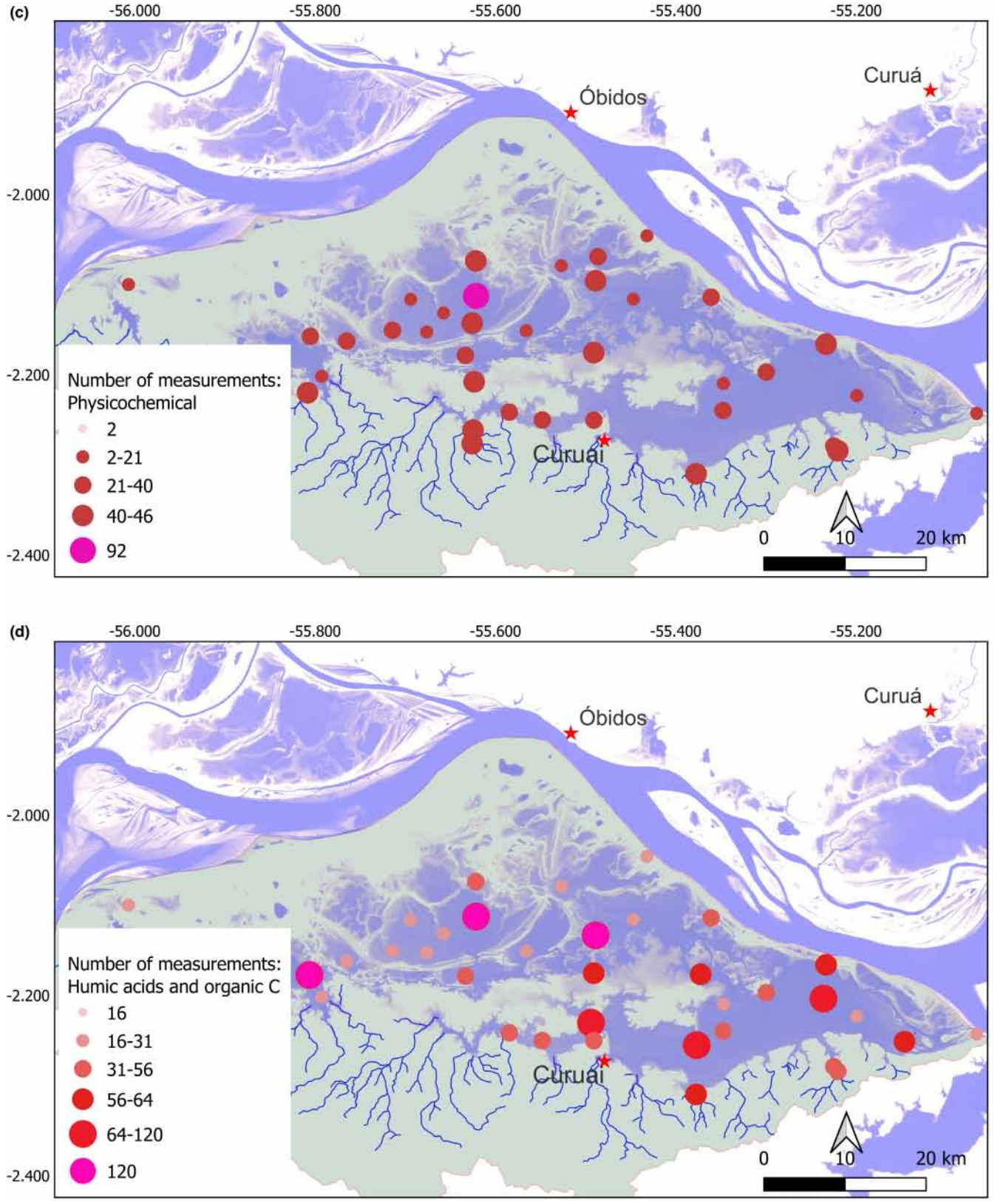

FIGURE 5 (Continued)

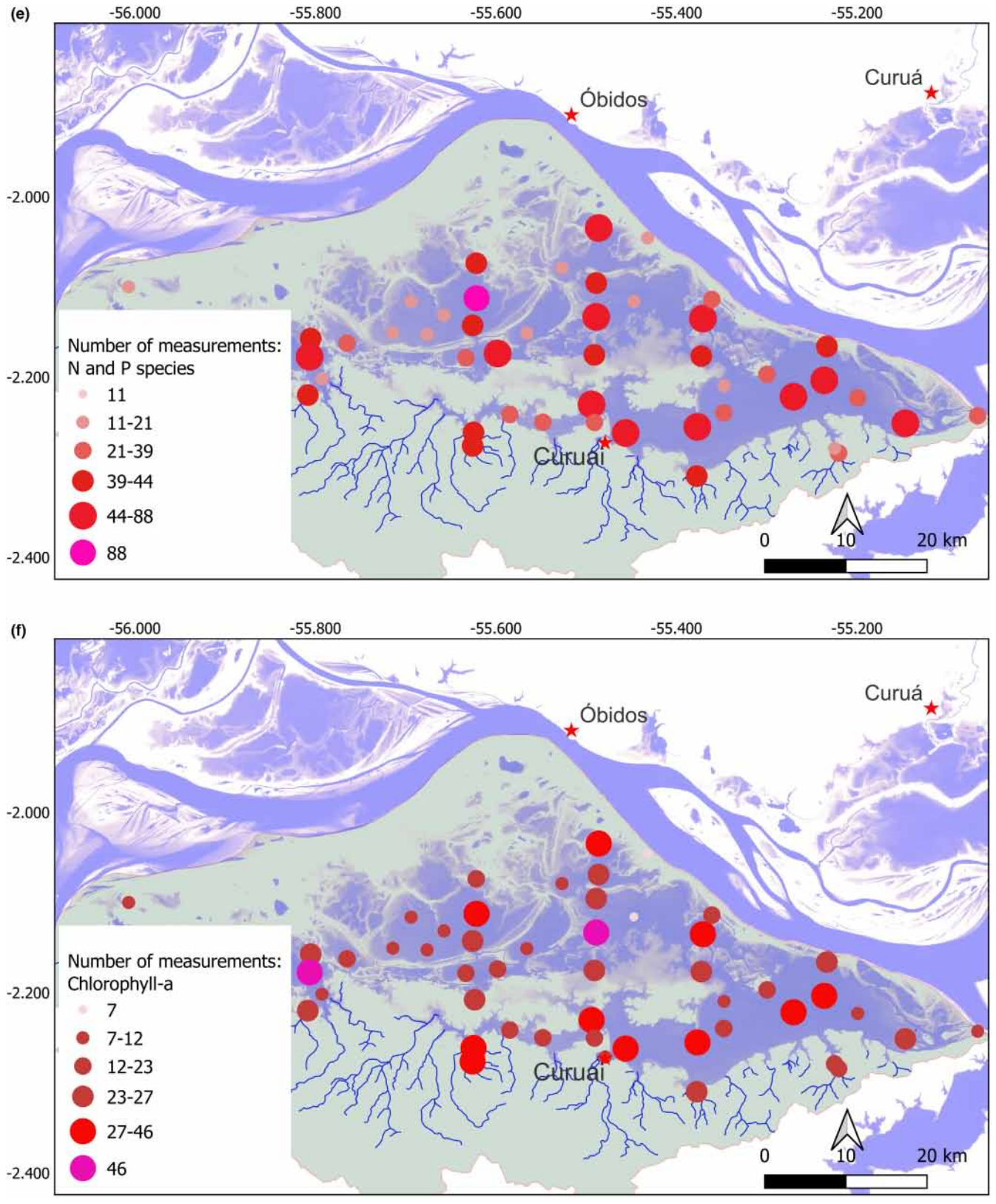

FIGURE 5 (Continued)

5.1 | Some recommendations for using the data set for comparison with data acquired in the past

Because of rainfall intensification since 2001 at the basin scale (Gloor et al., 2013), the maximum water levels attained each year during 2001–2016 are significantly higher than during the period 1983–2000. In contrast, the minimum levels achieved did not differ significantly between the two considered periods. But the rate of change during water level rising and falling (i.e. the variation in water level during a given period, namely January–April for rising, September–November for falling), varies significantly from one period to another. The water level rises and decreases faster during the 2001–2016 period compared to the 1983–2000 period (Arvor et al., 2018). Consequently, we recommend comparing the data considering water levels (available on the ANA website https://www.snirh.gov.br/hidroweb/serieshistoricas) and not only the hydrological periods.

The tidal area between low and high water is suitable for livestock grazing. Thus, the cattle transhumance between the upland and the floodplain each year. Variations in hydrological cycles from 1 year to the next consequently directly influence these activities in such floodplains (Bommel et al., 2016; Katz et al., 2020). Still, compared with older data, it is worth mentioning that livestock farming has increased considerably since the early 1990s, with potential impacts on water quality. The primary forest in these local basins has been gradually replaced by grazing land, providing shelter for livestock during the high-water seasons. Cultivated areas (mainly cassava and food crops for family production) are set aside at the end of a 4-year cycle to replenish the soil by allowing secondary vegetation (capoeira for the local population) to grow (Bommel et al., 2016). The evolution of land use based on the analysis and processing of Landsat images during the low-water periods in 1985, 1997 and 2014, validated by fieldwork, has been proposed (Peres et al., 2018). This study did show a decrease of at least 25% in primary forest (an increase of about 47% in secondary vegetation) between 1985 and 2014, but a slight variation between 1985 and 1997. It also shows an increase of about 26% in cultivated areas between 1985 and 1997, and their decline between 1997 and 2014 (18%), while the area of pastureland rose by about 37% during the same period. These results denote some important and relatively rapid shifts in agricultural activities and, consequently, important land cover changes that might affect the water quality and the water balance of the floodplain.

6 | CONCLUSION

The 5-year sample collection survey in the LGC floodplain provided information on the temporal and spatial water quality variability from a set of physical–chemical parameters and chlorophyll-a in surface waters. There were nine collection missions (between 2013 and 2017) in the different phases of the flood pulse: rising, high water, flushing and low water in the seven main floodplain lakes. The database is available at https://dataverse.ird.fr/dataverse/umr_espace-dev. Heritage data, new data and data from other floodplains will enrich this data set. The current data set has the potential to verify specific hypotheses about the biogeochemical functioning of floodplain lakes. Finally, it is also a benchmark of water quality in this type of environment and the transformations underway in the basin.

AUTHOR CONTRIBUTIONS

Derlayne Dias Roque: Data curation (lead); writing – original draft (lead). **Marie-Paule Bonnet:** Conceptualization (lead); data curation (equal); funding acquisition (lead); investigation (equal); methodology (equal); supervision (equal); writing – review and editing (equal). **Jérémie Garnier:** Conceptualization (lead); data curation (equal); funding acquisition (lead); investigation (equal); methodology (equal); supervision (equal); writing – review and editing (equal). **Cleber Nunes Kraus:** Methodology (equal); writing – review and editing (equal). **Patrick Seyler:** Conceptualization (equal); funding acquisition (supporting); methodology (equal); supervision (supporting); writing – review and editing (supporting). **David Da Motta Marques:** Conceptualization (supporting); data curation (supporting); funding acquisition (lead); methodology (equal); writing – review and editing (equal).

ACKNOWLEDGEMENTS

This research was funded by the FRB (*Fondation pour la recherche sur la biodiversité*) through the Clim-FABIAM research program, the CNPq (*Conselho Nacional de Desenvolvimento Científico e Tecnológico*, grant number 490634/2013-3), by IRD (*Institut de Recherche pour le Développement*) through the Joint international laboratory LMI OCE (*Laboratoire Mixte International Observatoire des Changements Environnementaux*) and by the French-Brazilian GUYAMAZON program through the Bloom-ALERT project. The works were partially supported by Europe through the MSCA – RISE ODYSSEA project and by the Brazilian project 'INCT ODISSEIA' (CNPq project number CNPq 465483/2014-3) and by the BONDS ('Balancing biodiversity conservation and development in Amazon wetlands') funded by through the 2017–2018 Belmont Forum and Biodiversa joint call under the BiodivScen ERA-net COFUND program, and with funding organizations French National Research Agency (ANR), Sao Paulo Research Foundation (FAPESP), National Science Foundation (NSF), The

research Council of Norway and the German Federal Ministry of Education and Research. The first author thanks the CAPES (*Coordenação de Aperfeiçoamento de Pessoal de Nível Superior*) for providing financial assistance. Jeremie Garnier was supported by CNPq grant 311430/2021-0.

CONFLICT OF INTEREST STATEMENT

The authors declare no conflict of interest.

OPEN RESEARCH BADGES

This article has earned an Open Data badge for making publicly available the digitally shareable data necessary to reproduce the reported results. The data is available at https://doi.org/10.23708/SNGQHV. Learn more about the Open Practices badges from the Center for Open Science: https://osf.io/tvyxz/wiki.

ORCID

Marie-Paule Bonnet https://orcid.org/0000-0002-3950-4041
Jérémie Garnier https://orcid.org/0000-0001-9571-7933
Cleber Kraus Nunes https://orcid.org/0000-0002-5116-3681
Patrick Seyler https://orcid.org/0000-0003-3390-0614
David Motta Marques https://orcid.org/0000-0002-3809-8053

REFERENCES

Alcântara, E., Stech, J., Novo, E., Shimabukuro, Y. & Barbosa, C. (2008) Turbidity in the amazon floodplain assessed through a spatial regression model applied to fraction images derived from MODIS/Terra. *International Geoscience and Remote Sensing Symposium (IGARSS)*, 46(10), 4550–4553. Available from: https://doi.org/10.1109/IGARSS.2007.4423869

APHA. (2012). *Standard methods for the examination of water and wastewater*. In: Rice, E.W., Baird, R.B., Eaton, A.D. & Clesceri, L.S. (Eds.) 22nd edn., Washington, D.C.: American Public Health Association (APHA), American Water Works Association (AWWA) and Water Environment Federation (WEF).

Arvor, D., Cabral, A., Simões, M. & Bonnet, M.P. (2018) Observatory of the dynamics of interactions between societies and environment in the amazon, ODYSSEA Project, D3.1 report, EU 691053. https://www.odyssea-amazonia.org/pt/produtos/deliverables/2018

Barbosa, C.C.F., de Moraes Novo, E.M.L., Melack, J.M., Gastil-Buhl, M. & Filho, W.P. (2010) Geospatial analysis of spatiotemporal patterns of pH, total suspended sediment and chlorophyll-a on the Amazon floodplain. *Limnology*, 11, 155–166.

Bomfim, E.D.E.O. (2017) *Indicadores biogeoquímicos de qualidade ambiental da várzea Lago Grande do Curuaí, Amazônia brasileira* [Universidade de Brasília].

Bomfim, E.O., Kraus, C.N., Lobo, M.T.M.P.S., Nogueira, I.S., Peres, L.G.M., Boaventura, G.R. et al. (2019) Trophic state index validation based on the phytoplankton functional group approach in Amazon floodplain lakes. *Inland Waters*, 9(3), 309–319. Available from: https://doi.org/10.1080/20442041.2019.1570785

Bommel, P., Bonnet, M.-P., Coudel, E., Haentjens, E., Nunes, C., Melo, G. et al. (2016) Livelihoods of local communities in an Amazonian floodplain coping with global changes. *IEMSs Proceedings*, 8.

Bonnet, M.P., Barroux, G., Martinez, J.M., Seyler, F., Moreira-Turcq, P., Cochonneau, G. et al. (2008) Floodplain hydrology in an amazon floodplain lake (Lago Grande de Curuaí). *Journal of Hydrology*, 349(1–2), 18–30. Available from: https://doi.org/10.1016/j.jhydrol.2007.10.055

Bonnet, M.P., Garnier, J., Barroux, G., Boaventura, G.R. & Seyler, P. (2016) Biogeochemical functioning of Amazonian floodplains: The case of Lago Grande de Curuai. In: *Riparian zones: characteristics, management practices and ecological impacts*. Pokrovsky, O.S., Viers, J. (Eds.), New York, NY: Nova Science Publishers, InC., pp. 77–98. ISBN 978–1–63484–613–4.

Bonnet, M.P., Pinel, S., Garnier, J., Bois, J., Resende Boaventura, G., Seyler, P. et al. (2017) Amazonian floodplain water balance based on modelling and analyses of hydrologic and electrical conductivity data. *Hydrological Processes*, 31(9), 1702–1718. Available from: https://doi.org/10.1002/hyp.11138

Bourgoin, L.M., Bonnet, M.P., Martinez, J.M., Kosuth, P., Cochonneau, G., Moreira-Turcq, P. et al. (2007) Temporal dynamics of water and sediment exchanges between the Curuaí floodplain and the Amazon River, Brazil. *Journal of Hydrology*, 335(1–2), 140–156. Available from: https://doi.org/10.1016/j.jhydrol.2006.11.023

Câmara dos Reis, M., Lacativa Bagatini, I., de Oliveira Vidal, L., Bonnet, M.-P., da Motta Marques, D. & Sarmento, H. (2019) Spatial heterogeneity and hydrological fluctuations drive bacterioplankton community composition in an Amazon floodplain system. *PLoS One*, 14(8), e0220695. Available from: https://doi.org/10.1371/journal.pone.0220695

Castello, L. & Macedo, M.N. (2016) Large-scale degradation of Amazonian freshwater ecosystems. *Global Change Biology*, 22(3), 990–1007. Available from: https://doi.org/10.1111/gcb.13173

Castillo, M.M. (2020) Suspended sediment, nutrients, and chlorophyll in tropical floodplain lakes with different patterns of hydrological connectivity. *Limnologica*, 82, 125767. Available from: https://doi.org/10.1016/j.limno.2020.125767

Davidson, N.C. (2014) How much wetland has the world lost? Long-term and recent trends in global wetland area. *Marine and Freshwater Research*, 65(10), 934. Available from: https://doi.org/10.1071/MF14173

Dias-Roque, D.F. (2022) *Análise das Influências Antrópicas Sobre o Funcionamento Biogeoquímico da Várzea de Curuái—Bacia Amazônica*. PhD thesis report. Brazil: Universidade de Brasília.

Forsberg, B.R., Melack, J.M., Dunne, T., Barthem, R.B., Goulding, M., Paiva, R.C.D. et al. (2017) The potential impact of new Andean dams on Amazon fluvial ecosystems. *PLoS One*, 12(8), e0182254. Available from: https://doi.org/10.1371/journal.pone.0182254

Frappart, F., Papa, F., Malbeteau, Y., León, J.G., Ramillien, G., Prigent, C. et al. (2015) Surface freshwater storage variations in the Orinoco floodplains using multi-satellite observations. *Remote Sensing*, 7(1), 89–110. Available from: https://doi.org/10.3390/rs70100089

Gloor, M.R.J.W., Brienen, R.J., Galbraith, D., Feldpausch, T.R., Schöngart, J., Guyot, J.L. et al. (2013) Intensification of the Amazon hydrological cycle over the last two decades. *Geophysical Research Letters*, 40(9), 1729–1733.

Gomes, L.F., Vieira, L.C.G., de Souza, C.A., Bonnet, M.P. & de Almeida, A.N. (2020) Environmental controls on zooplankton during hydrological periods of flooding and flushing in an Amazonian floodplain lake. *Limnetica*, 39(1), 35–48. Available from: https://doi.org/10.23818/limn.39.03

Gran, G. (1952) Determination of the equivalence point in potentiometric titrations. *Part II. Analyst*, 77(920), 661–671.

Hess, L.L., Melack, J.M., Affonso, A.G., Barbosa, C., Gastil-Buhl, M. & Novo, E.M.L.M. (2015) Wetlands of the lowland amazon basin: extent, vegetative cover, and dual-season inundated area as mapped with JERS-1 synthetic aperture radar. *Wetlands*, 35(4), 745–756. Available from: https://doi.org/10.1007/s13157-015-0666-y

IPBES, I. S.-P. P. on B. and E. S. (2019) *Summary for policymakers of the global assessment report on biodiversity and ecosystem services (Version summary for policy makers). Presented at the IPBES Plenary at its seventh session (IPBES 7, Paris, 2019), Zenodo*. https://doi.org/10.5281/zenodo.3553579

Jespersen, A.M. & Christoffersen, K. (1987) Measurements of chlorophyll-a from phytoplankton using ethanol as extraction solvent. *Archiv für Hydrobiologie*, 109, 445–454.

Katz, E., Lammel, A. & Bonnet, M.P. (2020) Climate change in a floodplain of the Brazilian Amazon: scientific observation and local knowledge. In: Welch–Devin, M., Sourdril, A. & Burke, B.J. (Eds). *Changing Climate, Changing Worlds: Local Knowledge and the Challenges of Social and Ecological Change*. Switzerland: Springer Nature, pp. 123–144. ISBN 978–3–030–37312–2.

Kraus, C.N. (2015) *Avaliação da estrutura da comunidade fitoplanctônica em várzeas amazônicas frente às variações hidrológicas, ambientais e espaciais*. Master thesis report, Brazil: Universidade de Brasília.

Kraus, C.N. (2019) *Dinâmica da comunidade fitoplanctônica e a dominância sazonal das cianobactérias na várzea de Curuai*. PhD thesis report, Santarém-PA: Universidade de Brasília.

Kraus, C.N., Bonnet, M., Nogueira, I.D.S., Morais, M.T., Marques, D.M., Garnier, J. et al. (2019) Unraveling flooding dynamics and nutrients' controls upon phytoplankton functional dynamics in Amazonian floodplain lakes. *Water*, 11(154), 1–17. Available from: https://doi.org/10.3390/w11010154

Kraus, C.N., Maciel, D.A., Bonnet, M.P. & Novo, E.M.L.M. (2021) Phytoplankton genera structure revealed from the multispectral vertical diffuse attenuation coefficient. *Remote Sensing*, 13(20), 4114. Available from: https://doi.org/10.3390/rs13204114

Latrubesse, E.M., Arima, E.Y., Dunne, T., Park, E., Baker, V.R., D'Horta, F.M. et al. (2017) Damming the rivers of the Amazon basin. *Nature*, 546(7658), 363–369. Available from: https://doi.org/10.1038/nature22333

Latrubesse, E.M., D'Horta, F.M., Ribas, C.C., Wittmann, F., Zuanon, J., Park, E. et al. (2020) Vulnerability of the biota in riverine and seasonally flooded habitats to damming of Amazonian rivers. *Aquatic Conservation: Marine and Freshwater Ecosystems*, 31, 1136–1149. Available from: https://doi.org/10.1002/aqc.3424

Lobo, M.T.M.P.S. (2016) *Dinâmica do fitoplâncton na várzea de Curuai (Pará, Brasil) durante a enchente e a vazante*. Master thesis report Brazil: Universidade Federal de Goiás – UFG.

Lobo, M.T.M.P.S. (2021) *Assembleias algais em uma várzea amazônica: influência do pulso de inundaçao*. PhD thesis report, Brazil: Universidade Federal de Goiás, UFG.

Lobo, M.T.M.P.S., de Souza Nogueira, I., Fabris Sgarbi, L., Nunes Kraus, C., de Oliveira Bomfim, E., Garnier, J. et al. (2018) Morphology-based functional groups as the best tool to characterize shallow lake-dwelling phytoplankton on an Amazonian floodplain. *Ecological Indicators*, 95, 579–588. Available from: https://doi.org/10.1016/j.ecolind.2018.07.038

Mackereth, F., Heron, J. & Talling, J. (1989) *Water analysis: some revised methods form limnologists*. Kendal: Titus Wilson and Son Limited.

Moreira-Turcq, P., Bonnet, M.P., Amorim, M., Bernardes, M., Lagane, C., Maurice, L. et al. (2013) Seasonal variability in concentration, composition, age, and fluxes of particulate organic carbon exchanged between the floodplain and Amazon River. *Global Biogeochemical Cycles*, 27(1), 119–130. Available from: https://doi.org/10.1002/gbc.20022

Novo, E.M.L.M. & Melack, J.M. (2013). LBA–ECO LC–07 Reflectance Spectra and Water Quality of Amazon Basin Floodplain Lakes. ORNL DAAC.

Pekel, J.F., Cottam, A., Gorelick, N. & Belward, A.S. (2016) High-resolution mapping of global surface water and its long-term changes. *Nature*, 540(7633), 418–422.

Peres, L.G.M., Gurgel, H. & Laques, A.-E. (2018) Dinâmica da paisagem em planícies de inundação amazônicas: O caso do Lago Grande do Curuai, Pará, Brasil. *Confins*, 35, 23. Available from: https://doi.org/10.4000/confins.13010

Renó, V.F., Novo, E.M.L.M., Suemitsu, C., Rennó, C.D. & Silva, T.S.F. (2011) Assessment of deforestation in the lower Amazon floodplain using historical Landsat MSS/TM imagery. *Remote Sensing of Environment*, 115(12), 3446–3456. Available from: https://doi.org/10.1016/j.rse.2011.08.008

Reis, M.C. (2017) *Dinâmica espaço-temporal do bacterioplankton em um sistema de inundação Amazônico*. Brasil: Universidade Federal de São Carlos, UFSCAR. Master thesis available at: https://repositorio.ufscar.br/handle/ufscar/9241

Roberto, M.C., Santana, N.F. & Thomaz, S.M. (2009) Limnology in the upper Paraná River floodplain: large-scale spatial and temporal patterns, and the influence of reservoirs. *Brazilian Journal of Biology*, 69(SUPPL. 2), 717–725. Available from: https://doi.org/10.1590/s1519-69842009000300025

Rodríguez, M., Steiger, J., Rosales, J., Laraque, A., López, J.L., Castellanos, B. et al. (2019) Multi-annual contemporary flood event overbank sedimentation within the vegetated lower Orinoco floodplain, Venezuela. *River Research and Applications*, 35(8), 1241–1256. Available from: https://doi.org/10.1002/rra.3510

Rudorff, C.M., Dunne, T. & Melack, J.M. (2018) Recent increase of river–floodplain suspended sediment exchange in a reach of the lower Amazon River. *Earth Surface Processes and Landforms*, 43(1), 322–332. Available from: https://doi.org/10.1002/esp.4247

Rudorff, C.M., Melack, J.M. & Bates, P.D. (2014a) Flooding dynamics on the lower Amazon floodplain: 1. Hydraulic controls on water elevation, inundation extent, and river-floodplain discharge. *Water Resources Research*, 50(1), 619–634. Available from: https://doi.org/10.1002/2013WR014091

Rudorff, C.M., Melack, J.M. & Bates, P.D. (2014b) Flooding dynamics on the lower Amazon floodplain: 2. Seasonal and interannual hydrological variability. *Water Resources Research*, 50(1), 635–649. Available from: https://doi.org/10.1002/2013WR014714

How to cite this article: Roque, D.D., Bonnet, M.-P., Garnier, J., Nunes, C.K., Seyler, P. & Marques, D.M. (2023) Surface water quality in Amazonian Floodplain Lakes, data set of the Lago Grande de Curuai Floodplain Lake, Pará-Brazil. *Geoscience Data Journal*, 00, 1–15. Available from: https://doi.org/10.1002/gdj3.207